Ocean and Sea Ice SAF

Scientific Report

SAF/OSI/CDOP/KNMI/SCI/RP/141

Development of a Global Scatterometer Validation and Monitoring

by

M. Portabella and A. Stoffelen

(July 2007)

Table of Contents

1 Introduction

Objective

Stoffelen (1998b) developed an advanced validation model for winds over the ocean based on triple collocation of scatterometer, buoy, and Numerical Weather Prediction (NWP)model winds. This method has been further tested in the tropical region for wind (*Djepa, 2001*) and been extended to wind stress modelling in the context of the Climate Monitoring (CM) Satellite Application Facility (SAF) (*Stoffelen et al, 2006*). In line with user and reviewer recommendations for further validation, we here report on the extension of this activity to the extra-tropics in an Ocean & Sea Ice (OSI)SAF Visiting Scientist (VS) study.

Wind forces motion in the ocean and in turn the motion in the ocean determines the weather and climate in large portions of the world. Wind forcing is essential in the El Niño Southern Oscillation (ENSO) and other ocean-atmosphere interaction phenomena, occurring in the Tropics. As such, a homogeneous wind data set of high quality would much advance research on the prediction and mechanisms of seasonal forecasting. *Vialard* (2000) emphasizes that wind stress is certainly the most important forcing in the tropics. Moreover, ocean circulation and ENSO play a key role in the Earth' climate. Besides tropical needs, obvious applications of such wind stress product would be among others in the modelling of the Antarctic circumpolar current, forcing of the southern oceans, research on the variability and occurrence of storms, and forcing in complex basins, e.g., the Mediterranean. Complementary to buoy observations, it would be useful to have continuous wind stress time series of high temporal and spatial resolution, extending beyond the buoy area. This would aid in the understanding of the unexplained variability of these wind events from year to year.

Therefore, a scatterometer ocean stress (SOS) product has been developed at KNMI within the framework of the CM SAF. Such product potentially provides continuous wind stress time series of high temporal and spatial resolution, extending beyond the TAO and PIRATA buoy area. An interesting output of this work is that the two surface layer models that have been tested, i.e. the LKB and the ECMWF models, behave very similarly in the Tropics. In contrast with the LKB model, ECMWF defines wind stress as sea-state dependent. As such, the extra-tropical regions, where there is substantial wind variability and fetch, are most appropriate to study such effect for wind and stress. Besides, obvious applications of wind or stress would be among others in the modelling of the Antarctic circumpolar current, forcing of the southern oceans, and research on the variability and occurrence of storms.

To extend the buoy wind validation globally, a triple collocation dataset, i.e., ERS scatterometer, buoy, and ECMWF data, outside the Tropics is generated. This provides a validation of the extra-tropical scatterometer wind product in addition to the validation by *Hersbach et al* (2006). Moreover, to study the effects of sea state on wind (stress) uncertainty, the already defined (in the Tropics) scatterometer wind-to-stress calibration can be used together with ECMWF wave age information. Also, the convenience of using either LKB or ECMWF surface layer model to compute stress needs to be further explored in order to provide a final recommendation for a global scatterometer wind-to-stress calibration.

Wind data sources

Wind information is available from conventional platform observations, such as ship or buoy. These systems measure the atmospheric flow at a measurement height that can vary between 4 m and 60 m, and are thus not a direct measure of surface 10-m wind nor stress. Stress computation requires the transformation of these winds by Planetary Boundary Layer (PBL) parameterisation schemes in order to represent the sea surface conditions. These PBL schemes and more in particular, the Surface Layer (SL) schemes embedded in the PBL schemes, have improved accuracy over the years (*Smith et al., 1992*; *Donelan et al., 1993*; *Taylor and Yelland*, 2001; *Bourassa*, 2006) although they still contain transformation errors.

Furthermore, buoy wind observations and, by implication, the NWP analyses that exploit these data use a fixed frame of reference. However, the wind stress depends on the difference of motion between atmosphere and ocean. *Kelly et al.* (2001) show that the ocean currents do produce a significant bias in the buoy-derived wind stress estimations. In contrast, they show that scatterometer observations provide a measure of the relative motion between atmosphere and ocean, and therefore can potentially provide accurate wind stress information.

Since the conventional systems represent sparse and local measurements, only temporally and spatially coarse climatologies can be computed. Several studies have shown that the response of an ocean model depends on whether the wind stress forcing is by Numerical Weather Prediction (NWP) analyses or by climatologies directly based on observation systems. Such responses depend on data general quality but also on the spatial structures resolved by an observation system or NWP model. *Stoffelen* (1998a) illustrates that the general accuracy of data depends on geographical region and here we will extend earlier tropical studies (*Stoffelen et al, 2006*) to the extratropics.

Several authors have pointed to the mesoscale wavenumber gap in NWP wind datasets (e.g., *Chelton et. al., 2004*; *Chelton and Schlax, 1996*; and *Stoffelen, 1996*). This gap is caused by the aforementioned sparse conventional observations at the sea surface, but also aloft since NWP data assimilation systems are 4-dimensional (4D) in nature and thus require 4D observations to achieve uniform quality. In fact, mesoscale atmospheric waves are poorly observed. Scatterometers, however, do have the capability to observe the surface component of such waves. Moreover, scatterometers provide information on the inertial scale of ocean models and thus can potentially provide essential information to drive ocean models (e.g., *Milliff, 2005*; *Chelton et al., 2004*; *Chelton and Schlax, 1996*).

How do we measure wind stress from scatterometers?

A scatterometer measures the electromagnetic radiation scattered back from ocean gravity-capillary waves and it is difficult to validate quantitatively the relationship between the roughness elements associated with gravity-capillary waves and the measurements. As such, empirical techniques are employed to relate microwave ocean backscatter with geophysical variables. Since the launch of the Earth Remote Sensing Satellites, ERS-1 (on 17 July, 1991) and ERS-2 (on 21 April, 1995), with on board the active microwave instrument (*Attema, 1991*) operating at 5.4 GHz (C band) numerous retrieval optimisations and validation studies have been carried out. Usually the retrieved products from satellite scatterometers are validated by collocation with NWP model

(e.g., European Centre for Medium Range Forecast, ECMWF) background winds, and/or buoy measurements (*Stoffelen, 1998a*). A multitude of wind observations is available at a reference height of 10 m, and as such scatterometer winds are traditionally related to 10m winds. For ERS scatterometers, the function that relates the 10-meter wind to the backscatter measurements, i.e., the Geophysical Model Function (GMF), and is used nowadays by ESA and KNMI for wind retrieval is the so-called CMOD-5 (*Hersbach et al., 2006*).

Stoffelen (1998a) shows that for varying ocean wind conditions, the backscatter measurements vary along a well-defined conical surface in the 3D measurement space, i.e., the measurements depend on two geophysical variables or a 2D vector. CMOD-5 indeed well explains the distribution of backscatter measurements in measurement space.

Chelton et al. (2001) and *Stoffelen* (2002) show a high correlation between scatterometer-retrieved winds and wind stress. In fact, scatterometers measure sea surface roughness (rather than 10-meter wind), which is highly correlated with the wind stress. So, if one collocates wind stress or its equivalent value at 10-meter height (i.e., 10-m neutral wind) to CMOD-5 winds and estimates their relationship, one would obtain a CMOD-5 stress model (or CMOD-5 neutral wind model) providing the same conical fits in 3D measurement space. For example, *Milliff and Morzel* (2001) use a 10-m neutral wind GMF to transform SeaWinds scatterometer winds to stress.

The problem is that wind stress observations, as computed from buoy or NWP models, are not perfect. As already mentioned, the SL schemes which convert buoy or NWP wind observations into wind stress observations, are inaccurate. Therefore, in order to define a scatterometer wind-speed[1]-to-stress transformation, we need to account for the uncertainties of all data sources.

Surface layer models

There are several SL models in the literature that could be used to compute wind stress from buoy observations and/or NWP output. Given the inaccuracy of such models, prior to transforming scatterometer winds to stress, we first take a close look at them and compare their performance. For such purpose, we pick two of the most commonly used models, i.e., the LKB model (*Liu et al., 1979*) and the ECMWF SL model (*Beljaars*, 1997), and compare them in section 3. Such intercomparison, however, does not provide an independent framework to assess the accuracy of the SL models.

Triple collocations

Stoffelen (1998b) shows that given a triple collocation dataset, e.g., scatterometer, buoy, and NWP observations, the uncertainty of the three observing systems can be uniquely determined, provided that one of the systems is used as reference for calibration (scaling) of the other two systems. As such, in section 4, we perform the triple collocation exercise as described by *Stoffelen* (1998b), using scatterometer winds as calibration reference, to assess the random accuracy and scaling properties of both buoy and NWP wind stress derived from the SL models.

[1] Note that the transformation only refers to wind and stress intensities since the direction of the air flow is assumed to be constant in the SL.

The triple collocation exercise is also used to investigate whether the ERS scatterometer-derived (CMOD-5) winds are closer to a 10-m neutral wind (uniquely related to the wind stress) rather than to 10-m real wind, given the uncertainties of the different data sources and SL models used in the triple collocation. A scatterometer wind-to-stress transformation is finally recommended in order to produce a stress product from ERS scatterometer winds. Finally, a summary of the work and recommendations for future developments are presented in section 5.

As a first step towards a global ERS wind validation, and given the crucial role of wind stress in the tropics, *Stoffelen et al.* (2006) have carried out a thorough analysis in such area, focusing on atmospheric stability and humidity effects. On the other hand, effects due to wave age or fetch are known to be relevant in the extra-tropics. The work presented here focuses on the extra-tropics and, as such, is complementary to the work reported by *Stoffelen et al.* (2006). In fact, section 3 of *Stoffelen et al.* (2006) is used as guidance and differences between the tropical and the extra-tropical analysis are highlighted.

2 Dataset

A triple collocation dataset for the year 1999 and 2000 is generated to carry out the work described in this report. The three observing systems used in this dataset are the ERS-2 scatterometer, the extra-tropical moored buoy dataset available from the Global Telecommunication System (GTS), and the ECMWF model.

KNMI produces the scatterometer wind and stress products within the EUMETSAT-sponsored OSI and Climate Monitoring (CM) SAFs, and develops the wind processing software in the Numerical Weather Prediction (NWP) SAF. In the framework of these SAFs, KNMI has developed an ERS scatterometer data processing (ESDP) package for the generation of operational wind products. As such, ERS-2 ESDP (version 1.0g) 10-m winds are used in this study.

Due to the initial problems to access extra-tropical moored buoy data online (see Appendix), buoy data distributed trough the GTS stream and archived at ECMWF are used instead. At ECMWF, most of the surface data over the oceans are archived in the form of hourly ship or drifting buoy data. The high quality surface wind observations, as obtained from dedicated meteorological moored buoys, are available from those records. However, before using the data for verification, care has to be taken to process the data to remove any erroneous observations. The original quality control was discussed in *Bidlot et al.* (2002). For this work, we are interested in using hourly observations; hence the averaging of the data was not performed as done originally in *Bidlot et al.* (2002). The automatic quality control is also supplemented by manual removal of outliers as found by visual inspection of the observations with respect to ECMWF model (done every month). Furthermore, a check on buoy positions was added to remove cases with erroneous positions or situations where the buoys were drifting. Note that, because of how the GTS data are encoded, the individual wind observations are only available to the closest m/s. Sadly, GTS data records do not contain information on the instrument height. This information was gathered from the different data providers and added to the data records. Especially, buoy anemometer height can vary from 2 to 15 m. In this study, only open ocean buoys from extra-tropical regions were considered. As shown in Figure 1, only a handful of buoys were selected from the three main data providers: the National Data Buoy Centre (NDBC), the Marine Environmental Data Service (MEDS), and the UK Met Office.

Hourly sea surface winds together with other surface layer relevant parameters, such as sea surface temperature (SST) and air temperature (T) are retrieved from the ECMWF GTS buoy data files. Additionally, first guess (FG) ECMWF ERA-40 lowest level (approximately 10 meter height) winds, T, specific humidity (q), pressure (p), SST, surface pressure (sp) and Charnock parameters are retrieved from the ECMWF MARS archive. FG winds do not contain the observations it is compared with in the triple collocation, such that the FG error and the observed wind errors may be assumed independent.

The triple collocations are performed in the following way. The ESDP collocation software is used to spatially and temporally interpolate the ECMWF ERA-40 forecast data to the ERS-2 scatterometer data acquisition location and time, respectively. Then the ECMWF-ERS dataset is collocated to the GTS buoy dataset using the following criteria: only observations separated less

than 25 km in distance and 30 minutes in time are included in the ECMWF-ERS-BUOY triple collocation dataset. In practice, most of the collocations are within 12.5 km and 10 minutes, thus considerably reducing the collocation error, i.e., uncertainty due to spatial and temporal separation between collocated observations.

To avoid uncertainties from unnecessary SL model height transformations, it seems appropriate to use wind datasets from a fixed height. In this respect, the ECMWF ERA-40 winds used in here correspond to the lowest model level, i.e., about 10 meter height. Since the GTS buoy dataset contains many different buoy systems with different observation heights, a compromise between the amount of buoys and the observation height spread is needed. In this report, only buoy stations with anemometer heights between 4 and 5 meters are considered. In total, we use data from 41 buoy stations (see Figure 1), which produced about 3300 collocations over the mentioned period.

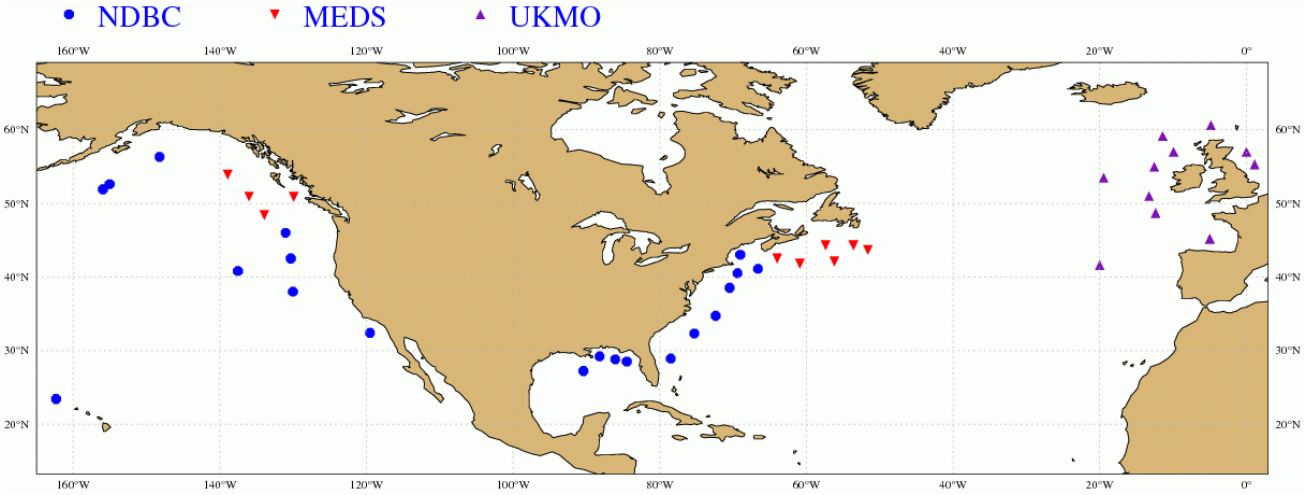

Figure 1. Geographical location of the GTS buoys.

Several Quality Control (QC) procedures have been applied to this dataset. The nominal ESDP QC procedure is applied to the ERS-2 retrieved wind dataset and only the GTS buoy data with the “highest quality” flag are used. Moreover, a 4-sigma test is performed to the triple collocated dataset as in *Stoffelen* (1998b). The tests are carefully designed in order to maintain the general shape of the wind PDFs.

3 SL models

Most of the equations that describe the physical balances and the turbulent budgets in the lowest 10% of the PBL, i.e., the surface layer, cannot readily be solved, due either to the presence of highly nonlinear terms or the requirement for enormous in-situ data bases (*Geernaert, 1999*). One can alternatively characterize the flow's dominant dynamic, geometric, and temporal scales, which involve characteristic time, space, or velocity scales, by dimensionless groups of variables. The similarity theory, first postulated by *Monin and Obukov* (1954), states that there exists such groups of variables which have functional relationships to the flow field and/or fluxes, and these in turn can be used to characterize the behavior of the higher order terms of the above mentioned equations.

The surface layer is assumed to be a constant flux layer and it extends up to a few tens of meters above the surface. In the bulk parameterization of the similarity theory, the fluxes are determined with the transfer coefficients which relate the fluxes to the variables measured, i.e.,

$$H = c \cdot \rho \cdot C_H (U - U_s) \cdot (T_s - T),$$

$$E = \rho \cdot C_E (U - U_s) \cdot (q_s - q), \qquad (1)$$

$$\tau = \rho \cdot C_D (U - U_s)^2,$$

where ρ and c are the density and isobaric specific heat of air; τ, H and E are the stress, heat and moisture fluxes; U, T and q are the wind speed, potential temperature and specific humidity at a reference height in the surface layer; U_s, T_s and q_s are the wind speed, temperature and specific humidity at the surface; and C_D, C_E and C_H are the transfer coefficients for momentum, heat and moisture, respectively. The C_D, also known as the drag coefficient, has been extensively studied. For deep water with large fetch, it has been expressed as a function of wind speed or assumed to be constant over a range of moderate wind speeds, e.g., *Businger*, (1975), *Garrat*, (1977). The transfer coefficients C_E and C_H are less well known and are usually treated as constants, and their variations with wind speed and stability neglected, e.g., *Pond et al.* (1974), and *Friehe and Schmitt* (1976).

The bulk transfer coefficients can be determined by integrating the U, T and q profiles. Close to the surface, the distributions of U, T and q are governed by diabatic processes. As such, the wind profile can be written as (e.g., *Businger 1973*):

$$u_* = \frac{k}{[\ln(\frac{z}{z_0}) - \psi(z/L)]} (U - U_s) \qquad (2)$$

where k is the von Karman constant, $u_*^2 = \tau / \rho$ is the friction velocity, z is the height above the surface, z_0 is the roughness length for momentum, ψ is the stability function for momentum (positive, negative, and null, for unstable, stable, and neutral conditions, respectively) and L is the Monin-Obukhov length, which includes the effects of temperature and moisture fluctuations on

buoyancy. Similar profiles to the one in Eq. 2 are also derived for the scale temperature (T_*) and the scale humidity (q_*) (see *Liu et al., 1979*). Since stability (z/L) depends on T and q, the set of 3 dimensionless profiles (u_*, T_*, and q_*) have to be solved at the same time.

In order to solve for u_*, the wind at certain height, among other parameters, is required (see section 3.1) and z_0 and L must be estimated (see Eq. 2). Once u_* is estimated, the SL models can be used to compute the wind at any height (within the SL) and any stability, e.g. neutral wind, just by modifying z and L, respectively, in Eq. 2. In other words, given a wind observation at certain height (within the SL), we can estimate the winds at any other height and stability, provided that we first go down to the surface and compute stress.

The discussion of air-sea transfer is not about the validity of the approach described above but generally about the details of parameter and function choices. As such, most SL models are based on Eqs. 1 and 2, and differences among them lie in the parameterization of L and/or z_0. This is the case for the two SL models used in this work, i.e., the LKB and the ECMWF SL models. Their similarities and differences are further discussed in the following section.

3.1 LKB versus ECMWF: formulation

The LKB and ECMWF SL models present the same roughness length function (see Liu et al., 1979, and Beljaars, 1997), which is written as:

$$z_0 = \frac{0.11 \cdot \nu}{u_*} + \frac{\alpha \cdot u_*^2}{g} \qquad (3)$$

where ν is the kinematic viscosity of the air (1.5×10^{-5} m^2/s), g is the gravitational constant of the Earth (9.8 m/s^2), and α is the (dimensionless) Charnock parameter (see *Charnock, 1955*). However, the Charnock value, which is a sea-state parameter, is substantially different, i.e., 0.011 for LKB and around 0.018 for ECMWF SL (the latter is not a fixed value).

The same happens with the formulation of the stability function $\psi(z/L)$, which is identical for both models, although the computation of the L parameter (Monin-Obukhov length) differs from one another (see Liu et al., 1979, and Beljaars, 1997).

The stand-alone ECMWF SL model uses as input U, T, q, pressure (p), observation height (z), SST, surface pressure (sp), and Charnock data. Similar input is used in LKB; the main difference is that no Charnock input but a default value of 0.011 is used instead. If q information is not available, LKB also allows relative humidity (rh) observations as input. Both SL models can solve for wind stress provided that U, T, and SST are available. That is, when humidity and pressure observations are not available, default values are used instead. Those values are slightly different, i.e., relative humidity (rh) of 0.8 and sp=1013 hpa for LKB versus rh=1 and sp=1000 hpa for ECMWF.

Another relevant aspect of these models is the convergence procedure the models use to solve for u_* (and T_* and q_*). That is, u_* depends on two unknowns, z_0 and ψ (see Eq. 2), which in principle are independent from one another. In other words, the roughness length, which directly depends

on the forcing (u_*) and the sea state (Charnock) as expressed in Eq. 3, should not be correlated with atmospheric stability (z/L). However, since the wind information available is always at certain height (z) above the surface, we need stability correction to go down to the surface and, as such, certain correlation between z_0 and z/L is inevitable. This is especially the case for LKB algorithm, which solves Eqs. 2 and 3 at the same time. In the case of ECMWF, the mentioned correlation is much smaller since z_0 (Eq. 3) is solved prior to z/L, making a set of assumptions about u_* and stability.

3.2 LKB versus ECMWF: results

In this section, we present some results of comparing the LKB model against the ECMWF SL model, using the extra-tropical dataset, i.e., GTS buoy data and the ECMWF data, described in section 2. These results are in general consistent with the results from *Stoffelen et al.* (2006), where a tropical dataset is used instead. Discrepancies between the two datasets are discussed below.

Figure 2 shows the two-dimensional histogram of LKB estimated u_* versus ECMWF SL estimated u_* for two different input datasets: GTS buoys (left plot) and ECMWF model output (right plot). Since the two datasets contain different parameters (see discussion in section 2) and the two SL models allow somewhat different input (see section 3.1), we select the coincident parameters for all 4 combinations: U, T, SST, and P. As it is clearly discernible, the distribution lies close to the diagonal, it is very narrow, and the correlation is 1, meaning that the estimated u_*

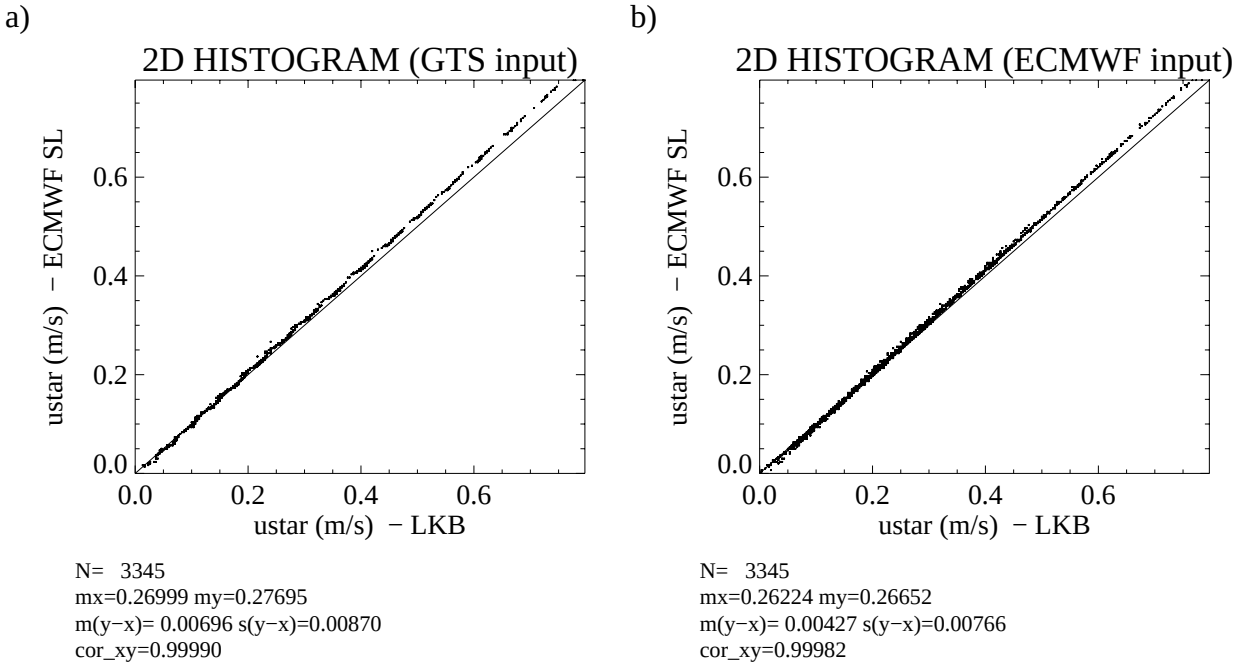

Figure 2. Two-dimensional histogram of LKB estimated u_* versus ECMWF SL estimated u_* for two different input datasets: GTS buoys (a) and ECMWF model output (b). N is the number of data; mx and my are the mean values along the x and y axis, respectively; m(y-x) and s(y-x) are the bias and the standard deviation with respect to the diagonal, respectively; and cor_xy is the correlation value between the x- and y-axis distributions.

is very similar, regardless of the SL model or the dataset used. In other words, the two models show very similar results.

A 5% bias at high u_* values needs to be explained, though. We know from earlier discussion that SL model differences must lie in the roughness length and the stability parameters. Therefore, we now take a closer look at them.

Roughness term

Figure 3 shows the same as Figure 2, but for the z_0 parameter. Again, the correlation between the two models is striking. However, we clearly see the differences between the two model formulations. As discussed in section 3.1, the Charnock parameter is substantially different for both models, i.e., 0.011 for LKB and 0.018 (default value) for ECMWF. Therefore, for very low u_* values, where the viscosity term (first right-hand side term of Eq. 3) is dominant, the distribution lies on the diagonal (same z_0 for both models), and for higher u_*, where the Charnock term is dominant (second right-hand side term of Eq. 3), the distribution is off diagonal, with a slope which is given by the ratio between the Charnock values of both models.

Looking at Figures 2 and 3, one can easily realize that in order to achieve such good agreement in u_* (Figure 2), the stability term in Eq. 3 has to compensate for the difference in the roughness term between the two models. Given the fact that the roughness term is logarithmic, the difference between LKB roughness term and ECMWF roughness term is just a constant, i.e.,

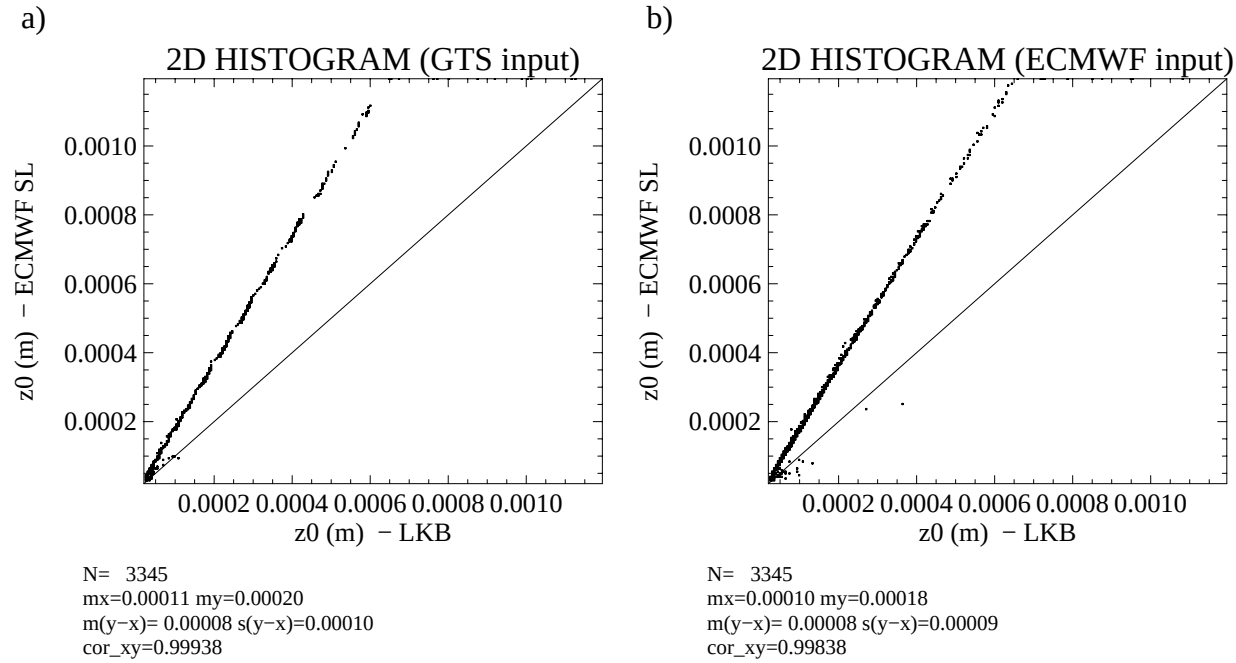

Figure 3. Same as Figure 2 but for the estimated z_0 parameter.

$\ln\left(\frac{z}{z_0^{ECMWF}}\right) = \ln\left(\frac{z}{z_0^{LKB}}\right) - k$, where $k = \ln(\frac{\alpha^{ECMWF}}{\alpha^{LKB}}) \cong 0.5$. Since the roughness term $\ln\left(\frac{z}{z_0^{LKB}}\right)$ values vary between 13 (low z_0) and 9 (high z_0), provided that the stability term is relatively small

in both models, there should be a bias of about 5% between ECMWF and LKB u_*, which is not present at low u_* values (see Figure 2).

Stability term

Figure 4 shows the ratio between the roughness term and the stability term as a function of z_0 for both the LKB model (left plot) and the ECMWF SL model (right plot). As already discussed in section 3.1, the correlation between z_0 and stability (z/L) is larger for LKB than for ECMWF SL model. This is actually shown in these plots (note that the left plot shows higher correlation than the right plot). The tropical dataset (*Stoffelen et al., 2006*) though shows larger correlation between z_0 and stability (z/L) and correlation difference between LKB and ECMWF SL model. The lower wind variability in the tropics as compared to the extra-tropics is the main reason for such an increase in the correlation scores. An interesting result here is that both plots show that the stability term is only relevant (ratio values lower than 10) for low z_0 values (i.e., low winds). This is consistent with the bias observed in Figure 2, i.e., the constant k becomes relevant at increasing z_0, since the stability impact becomes marginal and $\ln\left(\frac{z}{z_0^{LKB}}\right)$ decreases. We note from Figure 4 that LKB stability term is more relevant than the ECMWF stability term (i.e., the mean ratio value "my" is substantially smaller in the left plot than in the right one). Since most of the observations correspond to unstable ($\psi > 0$) situations (see Figure 5), the more relevant stability term for LKB compensates the larger z_0 values from ECMWF SL model, such that the resulting u_* values are very similar for both models.

Given the fact that both SL models use the same stability functions (ψ), we can easily prove that LKB estimates larger instability (higher negative z/L values) than ECMWF. Figure 5 shows the histogram of the stability parameter (z/L) for both the LKB model (solid line) and the ECMWF

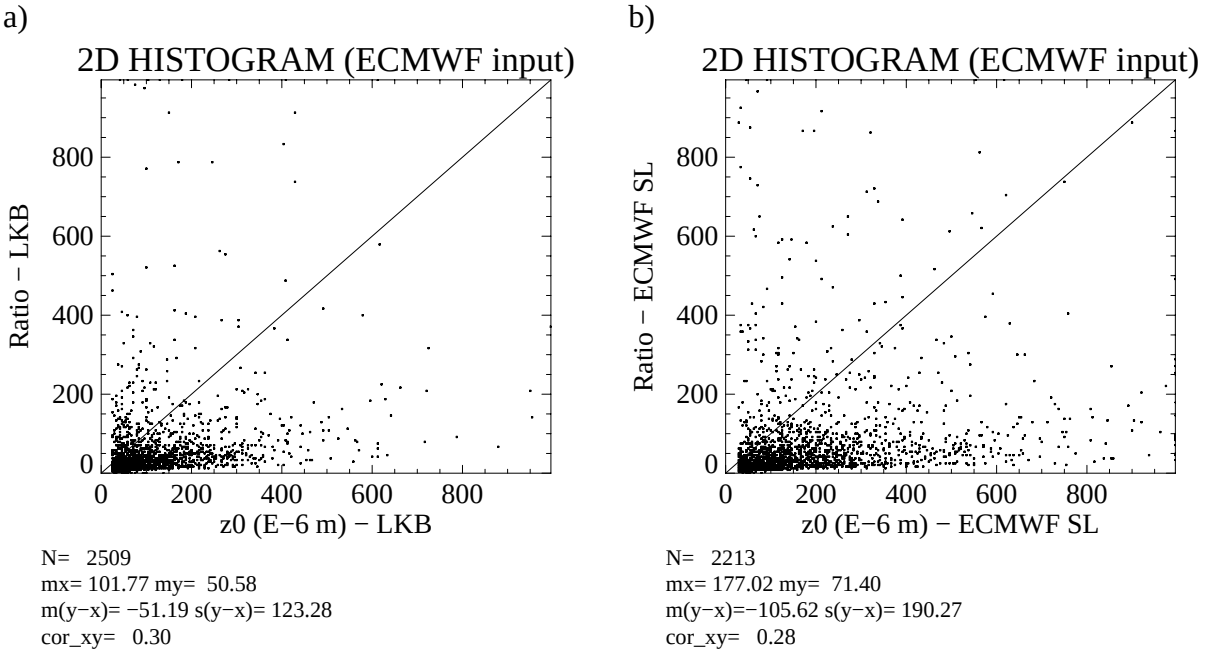

Figure 4. Ratio between the roughness term and the stability term as a function of z_0 for both the LKB model (a) and the ECMWF SL model (b). The legend is the same as for Figure 2.

SL model (dotted line). We note larger accumulations at increasing negative z/L values for LKB than for ECMWF SL, indicating larger estimated instability in the former model. Also note that the stability term is marginal for stable cases since these are close to neutral stability (i.e., no cases with large positive z/L).

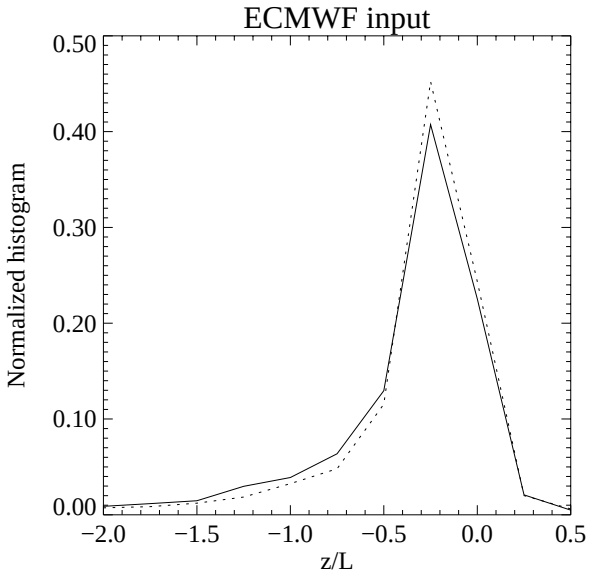

Figure 5. Normalized histogram of the stability parameter (z/L) for both the LKB model (solid) and the ECMWF SL model (dotted). Negative, null, and positive z/L values correspond to unstable, neutral, and stable stratification, respectively.

Sea state effect: Charnock parameter

The Charnock parameter is a measure of wave growth, hence wave age. As mentioned in section 3.1, the Charnock parameter is fixed for LKB but not for ECMWF SL model. The Charnock parameter, as formulated in the ECMWF Wave model (WAM) (see documentation at http://www.ecmwf.int/research/ifsdocs/CY28r1/Waves/), is a function of the so-called wave induced stress which in turn is function of the wind input source term (*Janssen, 2004*). Such Charnock output is included in the collocated ECMWF dataset (see section 2) and therefore can be used as input to the ECMWF SL model.

Up to now, results have been produced with fixed Charnock values (default values) for both models, i.e. 0.011 for LKB and 0.018 for ECMWF. Figure 6 shows a scatter plot of z_0 against u_*, as estimated by the ECMWF SL model, for GTS buoy (left plot) and ECMWF (right plot) input datasets. For the former dataset, no Charnock is provided and therefore the default value is used; for the latter dataset, variable Charnock (i.e., sea-state dependent) values are used. Note that the right plot (variable Charnock) shows more scatter than the left plot (fixed Charnock). As expected, the scatter in the right plot is also significantly larger than the scatter of the same plot but with the tropical dataset (see *Stoffelen et al., 2006*), confirming that the sea state is more relevant in the extra-tropics than in the tropics.

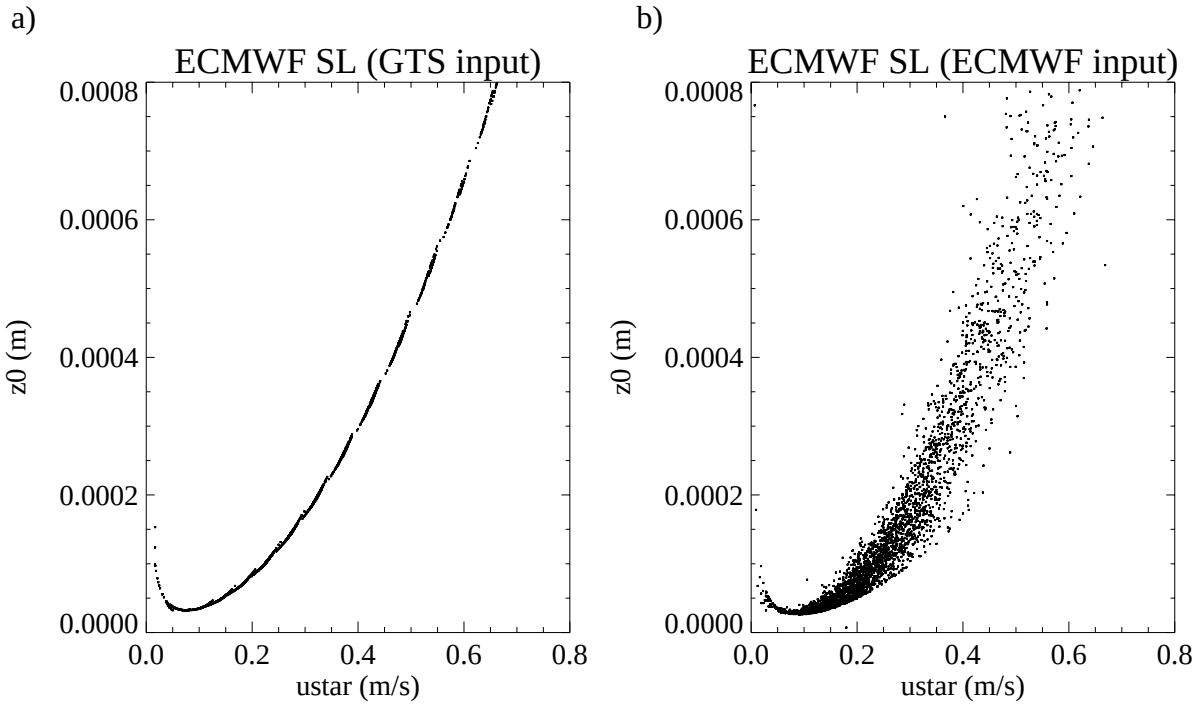

Figure 6. Scatter plot of ECMWF SL estimated z_0 against ECMWF SL estimated u_*, for GTS buoy (a) and ECMWF (b) input datasets. The latter contains variable Charnock values.

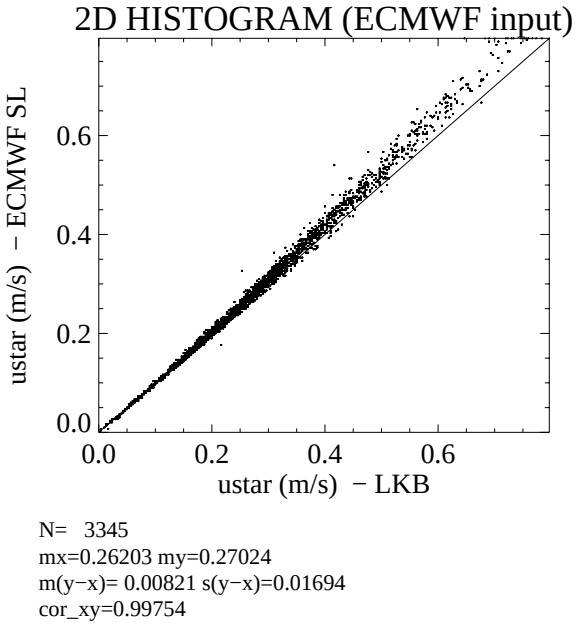

Figure 7. Same as Figure 2b but with variable Charnock input to the ECMWF SL model.

To show the impact of such scatter (i.e., sea state) on the estimated u_* uncertainty, Figure 2b is reproduced with (variable) ECMWF Charnock input. The 2-D histogram in Figure 7 shows only

larger spread than the one in Figure 2a, as indicated by the different Standard Deviation (SD) scores. However, as indicated by the correlation score in Figure 7 (very close to 1), the spread is relatively small. Even if the sea state is more relevant in the extra-tropics than in the tropics, it has little impact on the wind stress (u_*) estimation.

The triple collocated dataset can be used to better analyse the Charnock output from WAM. Figure 8 shows the scatterometer – ECMWF (left plot) and buoy – ECMWF (right plot) speed bias and SD as a function of the Charnock parameter. ECMWF and GTS buoy speeds have been converted to 4 m height speeds using ECMWF SL model. Since the scatterometer actually observes sea surface roughness, which is directly affected by the wave induced stress, one would expect that for increasing Charnock (sea state) values, sea surface roughness and therefore the mean biases in the left plot increase. However, the bias is rather flat and very similar to the one in the right plot, where for the same set of points no explicit roughness effect is expected. This is due to the fact that sea state is mainly wind-driven (note that if sea state is correlated to the wind vector cell or WVC wind, no bias is expected in the left plot) and cases of stress-wind decoupling are exceptional. The slight bias increase at large Charnock values in the left plot may be an indication of stress-wind decoupling, although there is not enough data to support this statement. It is therefore concluded that, in general, Charnock is very much correlated to the WVC wind and therefore has small impact in the quality of a global SOS[1]. However, the Charnock parameter may contain some added value for exceptional conditions such as cases of extreme wind variability and/or air-sea temperature difference. A much larger dataset is needed however to further investigate this.

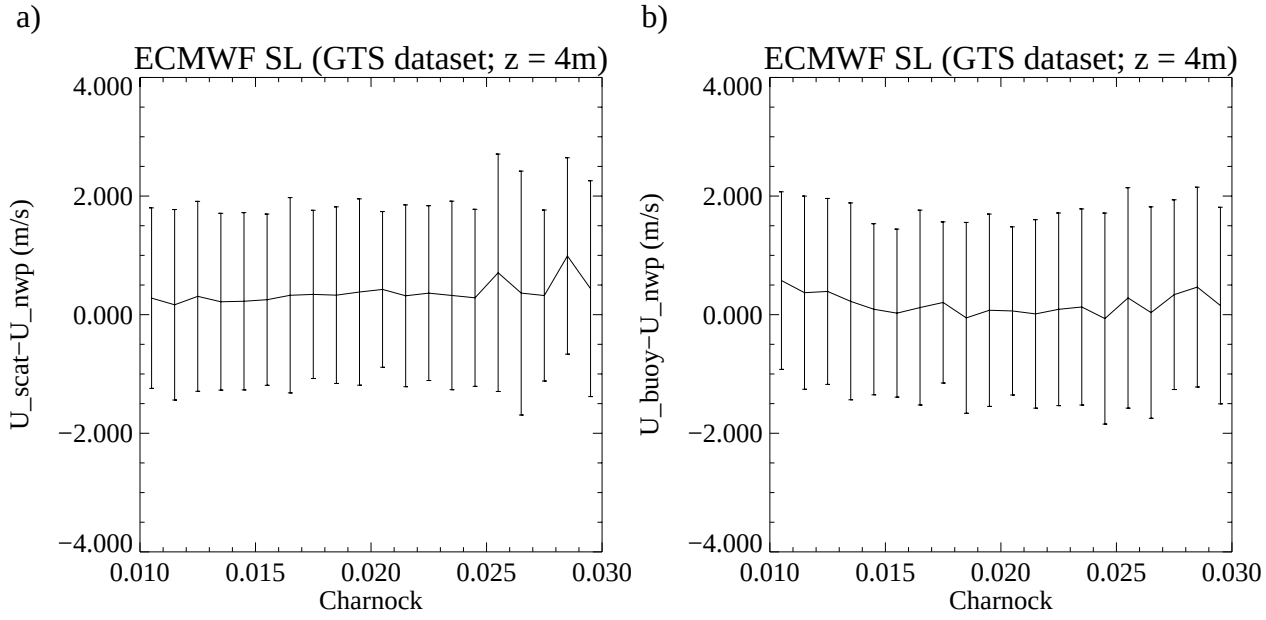

Figure 8. ERS scatterometer – ECMWF (left plot) and buoy – ECMWF (right plot) wind speed bias (solid curve) and SD (error bars) as a function of the Charnock parameter (bins of 1).

[1] Note that same conclusions are drawn when repeating the same exercise using calibrated (see section 4) scatterometer winds.

Neutral winds

The impact of stability on wind stress estimations is often measured by the difference between the actual wind (U) and its equivalent neutral wind (U_n), i.e., the wind that results from estimating u_*, given a wind observation at certain height z and under certain atmospheric stability (z/L), and using such u_* to solve Eq. 2 at the same height z assuming neutral stability (i.e., ψ=0).

Figure 9 shows the difference between U_n and U as a function of U using the LKB model, for GTS buoy (left plot) and ECMWF (right plot) input datasets. It is clear that the difference is comparable in both plots, indicating that both datasets produce similar stability effects. These effects are small, in the order of the surface current effects (within ±0.5 m/s). In the tropics (*Stoffelen et al., 2006*), differences between neutral winds and actual wind tend to increase for low winds (below 3 m/s) and then slightly decrease for increasing speeds. In the extra-tropics, this pattern is less evident, due to the presence of a wider range of stratification (stronger stable and unstable situations), although still present. The same pattern is produced when using ECMWF SL model instead of LKB (not shown). This is in contradiction with *Liu and Tang* (1996), who showed a 10% difference between neutral and actual winds, for winds between 4 m/s and 10 m/s, using the LKB model and GTS buoy input data. Further discussion on this matter can be found in *Stoffelen et al.* (2006).

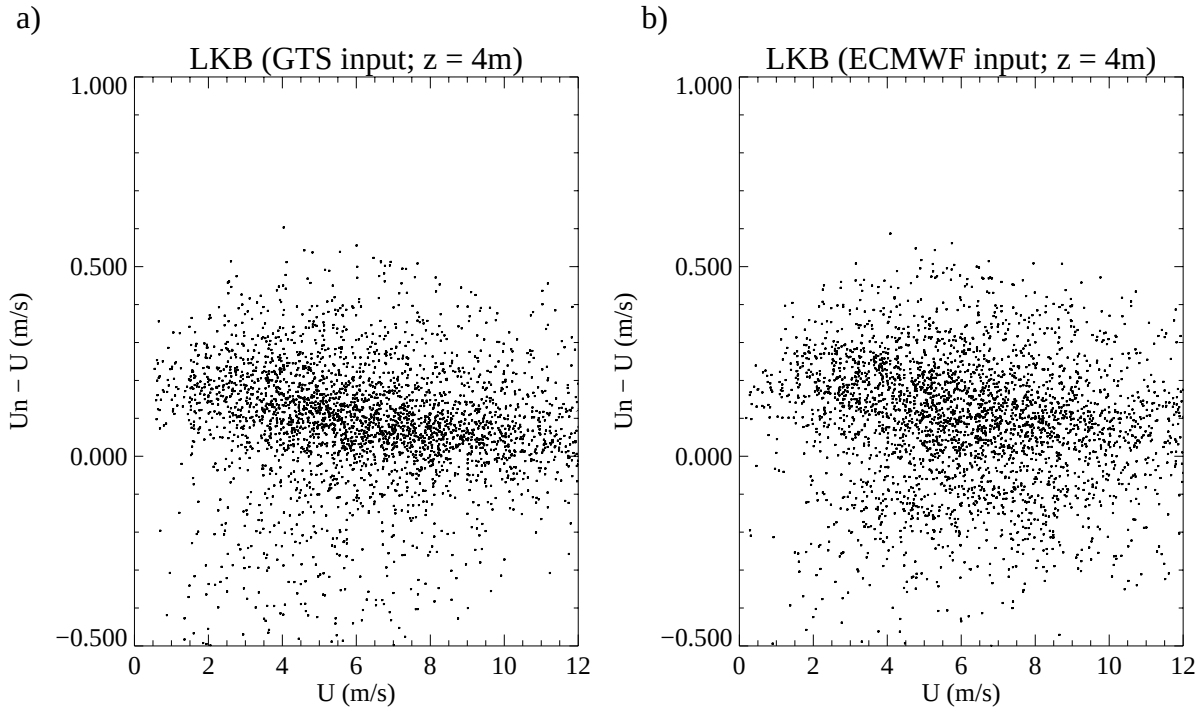

Figure 9. Difference between the LKB estimated U_n and U as a function of U, for GTS buoy (a) and ECMWF (b) input datasets, at 4 m height. Note that points from the left plot have been perturbed along the x-axis bins with a uniform distribution ranging [-0.5, 0.5] m/s to better discern the vertical distribution of points, i.e., the GTS speed binning (see section 2) otherwise produces a concentration of points along vertical lines.

In conclusion, LKB and ECMWF SL models produce very similar u_* values, except for high winds, where a 5% bias of the latter with respect to the former is found. The differences in the roughness parameterization are somewhat compensated by differences in the stability parameterization, except for high winds, where the stability term is negligible as compared to the roughness term. Differences between the (non sea state dependent) LKB and the (sea state dependent) ECMWF SL are tested in the extra-tropics, where sea state is substantially rougher than in the tropics, and found small.

4 Triple collocation exercise

In remote sensing, validation or calibration activities can only be done properly when the full error characteristics of the data are known. In practice, the problem is that prior knowledge on the full error characteristics is seldom available. *Stoffelen* (1998b) shows that simultaneous error modeling and calibration can be achieved by using triple collocations.

When the three observing systems represent the same spatial scales, the triple collocation procedure can resolve the uncertainty of the three systems, provided that one of them is used as reference for calibration. When the systems do not represent the same resolution, we have to take into account the spatial representativeness error[1]. In particular, we need to make an assumption on the correlation of the spatial representativeness error, i.e., the (true) variance common to the two systems that can resolve the smaller scales[2].

In our case, we have one system, i.e., ECMWF, that can only resolve large scales (> 200 km) and two systems, i.e., buoy and scatterometer, that can resolve smaller scales. Since the scatterometer resolves wind scales of about 50 km, the true variance on spatial scales of 50 to 200 km is resolved by both scatterometer and buoys, but not by ECMWF. For three similar observing systems to the ones used in this work, i.e., the National Oceanic and Atmospheric Administration (NOAA) buoy winds, ERS scatterometer winds, and National Centers for Environmental Prediction (NCEP) model winds, *Stoffelen* (1998b) estimated a correlated representativeness error (r^2) of 0.75 m^2/s^2 in the extra-tropics. We therefore assume such r^2 value for the 50-to-200 km scale true variance.

4.1 Error assessment using LKB and ECMWF SL models

As mentioned in section 1, we can use the triple collocation exercise to assess the performance of the two SL models that we have compared in section 3, i.e., LKB and ECMWF. That is, we use the SL models to convert GTS buoy and ECMWF wind observations to any reference height (e.g., 4 m, 10 m) and then estimate the errors of such buoy and NWP converted wind "observations", using ERS scatterometer CMOD-5 winds as reference system for calibration.

Table 1 shows the true variability and the observation error for each dataset, when LKB is used to produce the (buoy and NWP) wind datasets at 10-m (and 4-m) height. Note that the scores are given in terms of wind component SD rather than wind component variance (square of SD value) since the former is most commonly used to refer to wind variability and observation errors. The true variability (5.14 m/s and 5.43 m/s SD for u and v components, respectively) is comparable to the extra-tropical values estimated by *Stoffelen* (1998b) (4.68 m/s and 5.24 m/s SD for u and v

[1] When comparing two observation systems with different resolution, the variability of the higher resolution system at the scales that are not resolved by the lower resolution system may be interpreted as error, i.e., the spatial representativeness error. In fact, this variability is resolved true variance of the higher resolution system.
[2] This common variance is, in fact, the resolved true variance embedded in the representativeness error of both systems.

components, respectively) and substantially larger than the tropical values found by *Stoffelen et al.* (2006) (3.12 m/s and 4.89 m/s SD for u and v components, respectively). This is an expected result since there the wind variability is known to be substantially lower in the tropics than in the extra-tropics.

The correlated part of the representativeness error, as mentioned above, represents the common variance in the higher resolution systems, i.e., the scatterometer and the buoys. Therefore, when performing data interpretation for high resolution applications, e.g., development of 25-km or 50-km wind products, this common variance is considered as part of the true variance as well as part of the error (lack of high-resolution information) of the lower resolution system, i.e., NWP model. Table 2 accounts for such interpretation. However, when looking at lower resolution applications, e.g., NWP data assimilation, this common variance cannot be resolved and is therefore interpreted as part of the (spatial representativeness) error of the higher resolution systems, i.e., scatterometer and buoy. Note that Table 1 shows the same as Table 2 but accounting for the latter interpretation. We also note that differences between the two tables are produced by the assumed r^2 value, which is small compared to true variance but more significant compared to the error (variance) values.

When ECMWF SL model is used (instead of LKB) to produce the (buoy and NWP) wind datasets at 10-m height, the triple collocation results (not shown) are almost identical to the ones in Tables 1 and 2. That is, the performance of both SL models is comparable.

Table 1 Estimates of the wind component SD of the true distribution and the errors of the scatterometer, LKB-derived 10 m (4 m) buoy and ECMWF winds, for NWP-scale (~200 km) wind.

	True wind	Scatterometer	Buoy	ECMWF
u component (m/s)	5.14 (5.15)	1.53 (1.52)	1.32 (1.33)	1.28 (1.28)
v component (m/s)	5.43 (5.44)	1.31 (1.30)	1.48 (1.48)	1.23 (1.23)

Table 2 Same as Table 1, but for 50-km scale wind.

	True wind	Scatterometer	Buoy	ECMWF
u component (m/s)	5.22 (5.22)	1.26 (1.25)	0.99 (1.00)	1.55 (1.55)
v component (m/s)	5.50 (5.51)	0.98 (0.96)	1.19 (1.20)	1.50 (1.50)

The same exercise is repeated using buoy and NWP winds at 4 m height. The results (see values in brackets in Tables 1 and 2) are very similar in terms of true variability and errors of the different sources, also denoting the similar performance of both SL models. These results are in line with the results of section 3, where both models were showing little differences.

However, when performing triple collocation, the scaling factor for buoy (i.e., the buoy-to-scatterometer wind calibration value) is closer to one at a reference height of 4 m than at 10 m, meaning that CMOD5 scatterometer winds should be interpreted as 4-m winds rather than 10-m winds.

Table 3 Estimates of the wind component SD of the true distribution and the errors of the scatterometer, LKB-derived 10 m (4 m) buoy and ECMWF neutral winds, for NWP-scale (~200 km) wind.

	True wind	Scatterometer	Buoy	ECMWF
u component (m/s)	5.15 (5.15)	1.51 (1.52)	1.35 (1.34)	1.28 (1.28)
v component (m/s)	5.44 (5.44)	1.27 (1.27)	1.49 (1.49)	1.23 (1.23)

Table 4 Same as Table 3, but for 50-km scale wind.

	True wind	Scatterometer	Buoy	ECMWF
u component (m/s)	5.22 (5.22)	1.23 (1.25)	1.03 (1.03)	1.55 (1.55)
v component (m/s)	5.51 (5.51)	0.93 (0.93)	1.22 (1.21)	1.50 (1.50)

4.2 Scatterometer wind interpretation

As discussed in the introduction, scatterometers are essentially observing wind stress. Therefore, one may expect scatterometer-derived winds to be interpreted as equivalent neutral winds (i.e., stress) rather than real winds. In this section, we investigate the interpretation of scatterometer data by performing the triple collocation exercise for two different datasets:

a) ERS CMOD-5 winds, GTS buoy real winds, and ECMWF real winds;

b) ERS CMOD-5 winds, GTS buoy neutral winds, and ECMWF neutral winds.

The first dataset is the same as the one used in section 4.1. The second dataset is the same as the first one but for buoy and NWP converted neutral winds using either LKB or ECMWF SL model.

The true variability and error scores of dataset a) (see Tables 1 and 2) are very similar to the scores obtained with dataset b) (see Tables 3 and 4), when using LKB model and 10-m or 4-m height conversion. The same conclusions are drawn when using ECMWF SL model. This

indicates that scatterometer winds can explain the same true variability regardless of whether these are tested against real or neutral winds. The only significant difference between the two datasets results is in the scaling factor value[1], meaning that provided that we use the appropriate scaling in the scatterometer GMF (e.g., CMOD-5), scatterometer winds are as close to real winds than they are to equivalent neutral winds (or stress).

In order to reinforce such conclusion, and given the fact that CMOD-5 GMF was tuned to 10-m real (NWP) winds, we develop a new GMF (CMOD-5n) by tuning our CMOD-5 real winds to neutral winds. Figure 10 shows the bias of CMOD-5 winds with respect to 10-m buoy real winds (solid) and 10-m buoy neutral winds (dotted) as a function of wind speed. By subtracting these two curves, i.e., about 0.1 m/s, we can derive a real-to-neutral scaling (dashed) that can be used to convert CMOD-5 into CMOD-5n.

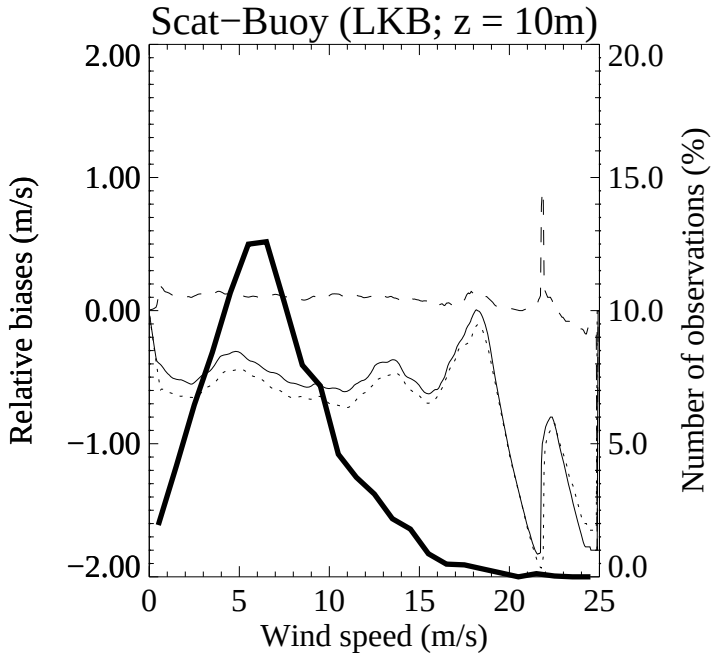

Figure 10. Relative bias of CMOD-5 winds with respect to 10-m buoy real winds (solid) and 10-m buoy neutral winds (dotted) as a function of wind speed. The buoy height conversion is performed with LKB model. The dashed curve corresponds to the solid minus the dotted curve. The thick solid curve corresponds to the number of data.

We then perform the same triple collocation exercise as before but using ERS CMOD-5n winds instead of CMOD-5 winds in datasets a) and b). As expected, the results are again very similar.

The fact that scatterometer winds are as close to real winds as to neutral winds can be explained as follows: on the one hand, the stability effects are small, i.e., differences between real and neutral winds are subtle (see Figure 9 in section 3.2); on the other hand, SL models and the different observations (wind, SST, air temperature) used by the models to compute height

[1] Since most of the times the extra-tropics present unstable stratification (see Figure 5), the real winds are biased low with respect to the equivalent neutral winds at any reference height within the SL.

conversions and neutral winds contain errors, which in turn mask the already subtle differences between real and neutral winds.

Although scatterometer winds can be interpreted as real winds from a statistical point of view, there may be special air-sea interaction situations where the scatterometer shows its real potential to measure stress. For example, note that *Stoffelen et al* (2006) found a difference value of 0.2 m/s between neutral and real winds with a tropical data set. The extra-tropical difference (i.e., 0.1 m/s) is smaller mainly because of cases with stable stratification that appear below the main cloud of points in Figure 9. For these single cases, the use of stability information may increase the true variability in a triple collocation exercise, therefore indicating that such scatterometer observations should be interpreted as neutral winds (or stress) rather than real winds. To prove this, further tests with a larger dataset are required.

4.3 Scatterometer wind-to-stress transformation

In order to obtain stress, first a well-calibrated scatterometer 10-m neutral wind is required. Then a SL model like LKB or ECMWF SL can be used to convert 10-m neutral winds to wind stress. In fact, since the most recently developed SL models (*Taylor and Yelland, 2001*; *Bourassa, 2006*) have similar performance up to 16 m/s (*Bourassa, 2006*), either one of them can be used to do the neutral-to-stress conversion. Since no stability information is needed to do this conversion, an independent scatterometer stress (SOS) product can be developed straightforwardly.

To obtain the calibrated scatterometer 10-m neutral wind, a scatterometer-to-buoy correction (calibration) and a real-to-neutral wind conversion need to be applied to CMOD-5 winds. The combined correction and conversion is represented by the dotted curve in Figure 10 and has a mean (absolute) value of 0.55 m/s, further confirming the results from *Hersbach et al.* (2006) with a similar extra-tropical dataset. However, it differs somewhat from the combined correction value of 0.8 m/s found by *Stoffelen et al.* (2006) doing the same triple collocation exercise but with a tropical dataset.

Several effects may lead to these differences between tropical and extra-tropical datasets. The most relevant are, on the one hand, the large wind variability in the extra-tropics, and, on the other hand, the effect of currents in the tropics. In order to recommend a final combined correction value, an analysis of the uncertainties of the triple collocation exercise (mainly produced by the mentioned effects) is performed. One way to analyze such uncertainties is to take the calibrated dataset (after triple collocation) and examine the residual biases buoy by buoy, i.e., scatterometer wind bias versus buoy and/or versus ECMWF at a particular buoy location. Table 5 shows the average and SD of the residual biases per buoy, for extra-tropical buoys with more than 50 collocations. The uncertainty found (SD of about 0.2 m/s) is consistent with the expected wind variability effect. A comparable result to that of Table 5 is found by *Stoffelen et al.* (2006) with a tropical dataset, indicating that the uncertainties produced by, e.g., the currents in the tropics are comparable to the ones produced by, e.g., the large wind variability in the extra-tropics. In other words, for a global correction both combined correction values (i.e., 0.8 m/s found in the tropics and 0.55 m/s in the extra-tropics) have a similar degree of confidence.

Therefore, we recommend adding 0.7 m/s (compromise between the tropical and the extra-tropical values) to CMOD-5 winds to obtain the scatterometer 10-m neutral winds. To obtain real winds we recommend adding 0.5 m/s to CMOD5.

Table 5 Average and SD of wind component residual biases (after wind calibration) per buoy location, for buoy and ECMWF winds against scatterometer winds.

	Buoy-Scat. U comp.	Buoy-Scat. V comp.	ECMWF-Scat. U comp.	ECMWF-Scat. V comp.
BIAS (m/s)	0.03	-0.12	0.08	-0.06
SD (m/s)	0.16	0.24	0.26	0.24

5 Summary and recommendations

5.1 Summary

Stoffelen et al. (2006) look for the most appropriate scatterometer wind-to-stress transformation, in order to produce a SOS product. For such purpose, a one-year (2000) triple collocated tropical dataset is used, i.e., ERS-2 scatterometer winds, TAO/PIRATA buoy data, and ECMWF model output. To validate such work and, in particular, to study the impact of large wind variability and waves on the wind-to-stress transformation, the work of *Stoffelen et al.* (2006) is repeated here using an extra-tropical dataset this time. In particular, two years (1999 and 2000) of extra-tropical triple collocations of ERS-2 scatterometer winds, GTS buoy data, and ECMWF model output is used.

First, a comparison between two commonly used SL models, i.e., LKB and ECMWF, is performed. The main difference between the two models is in the roughness length (z_0) and the stability (L) parameterizations. On the one hand, whereas LKB uses a constant Charnock value, ECMWF uses a substantially larger Charnock value. Since the ECMWF roughness parameterization is sea state dependent, its Charnock parameter is moreover variable, in particular in the extra-tropics.

On the other hand, LKB has larger instability (larger negative z/L values) with respect to ECMWF. This difference actually compensates for the difference in the roughness formulation for low and medium winds, such that the resulting stress values are very similar for both models. At high winds though, the stability term is much smaller than the roughness term and therefore the different roughness formulation results in some small stress bias between the two models.

Another relevant result of this comparison is that the bias due to the difference in the default Charnock values of both models remains the same when variable Charnock input is used for ECMWF SL model, and although the SD of the difference between LKB and ECMWF estimated stress increases somewhat, the correlation is very close to 1, indicating that Charnock (sea state) effects are rather small in terms of stress.

A triple collocation exercise based on *Stoffelen* (1998b) is then conducted to assess the performance of the LKB and the ECMWF SL models. For such purpose, we use the SL models to estimate wind at different reference heights from the buoy and NWP datasets. For every SL model, we therefore generate two new buoy and NWP stress datasets (at each height), which are combined with the scatterometer winds (using the latter as reference for calibration) to estimate their individual errors. The results show that the uncertainty in the NWP wind dataset is smaller than in the buoy wind dataset, but depending on the spatial scales of interest. They also show a similar performance of both SL models. This is not surprising since most of the recently developed SL models (e.g., *Taylor and Yelland, 2001*; *Bourassa, 2006*) produce a similar stress for surface winds below 16 m/s (*Bourassa, 2006*).

The same triple collocation exercise is repeated but equivalent neutral buoy and NWP winds are used instead of real winds. True variability and error scores are almost identical to the ones of the

previous exercise, and only scaling factors differ, meaning that scatterometer winds are as close to real winds than to neutral winds, provided that we use the appropriate scaling. A neutrally-scaled CMOD-5, i.e., CMOD-5n, is then derived, and CMOD-5n winds are used instead of CMOD-5 winds in the triple collocation exercise. The results confirm the duality in the interpretation of scatterometer winds. An explanation for this duality is that the already small stability effects (see section 3.2) are masked by the uncertainty in SL models and their inputs.

5.2 Recommendations

The results presented in this report confirm the ones obtained by *Hersbach et al.* (2006) with a similar extra-tropical dataset. Moreover, they validate the ones obtained by *Stoffelen et al.* (2006) with a tropical dataset. As such, we confirm that an independent ERS scatterometer stress (SOS) product can be obtained by adding 0.7 m/s to CMOD-5 wind and use such result as the 10-m neutral wind input to a recently developed SL model, which is needed to compute stress. [Note that KNMI uses LKB SL model since it is widely used and publicly available.]. A schematic illustration of the wind-to-stress conversion is shown in Figure 11.

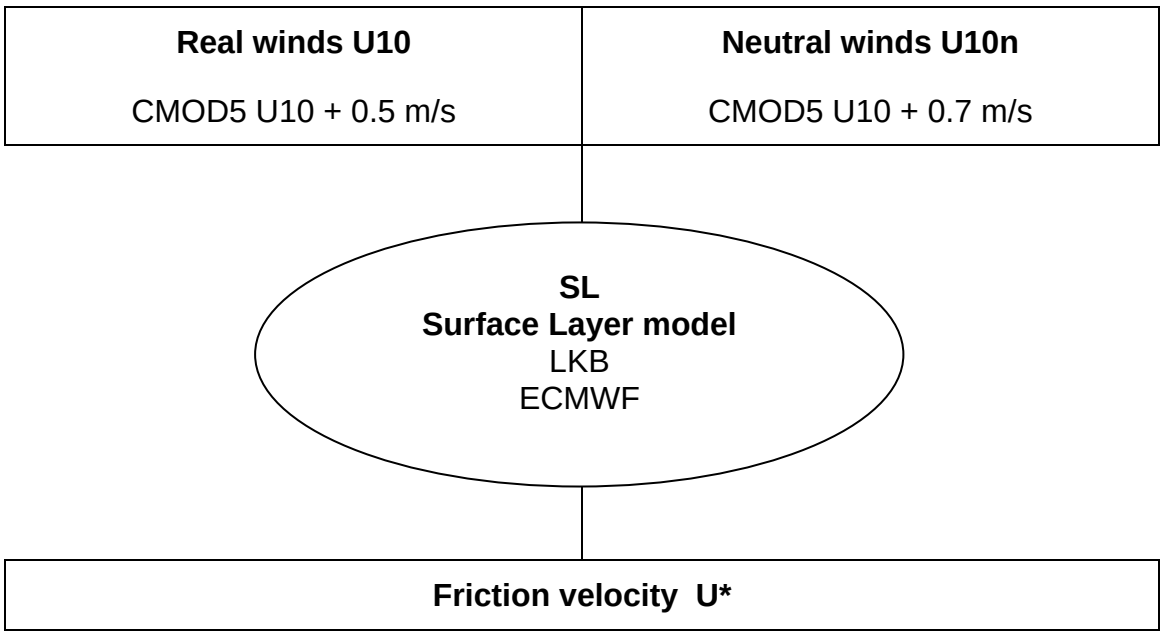

Figure 11. Schematic of recommended scatterometer wind and stress conversion. The well-validated CMOD5 winds at 10m height are used as basis for geophysical conversion to friction velocity. Either real or neutral 10m winds may be transformed to friction velocity by either LKB, ECMWF or any other similar SL model.

The formulation of the roughness length (Eq. 3) presented by these two SL models is not the only one available. Differences between different formulations have been thoroughly studied. For example, *Bonekamp et al* (2002) show that a wave age dependent Charnock SL model (such as ECMWF) is marginally better than a constant Charnock model (such as LKB). As such, several

authors have proposed different wave age dependent parameterizations, e.g., *Donelan* (1990), *Maat et al.* (1991), *Smith et al.* (1992), *Johnson et al.* (1998), and *Drennan et al.* (2003).On the other hand, *Yelland et al.* (1998) claimed that while, with increasing wind speed, waves typically become younger and rougher, it is difficult, at any given wind speed, to detect a clear relation between wave age and roughness. In line with this work, *Taylor and Yelland* (2001) proposed an alternative wave steepness parameterization of z_0. *Drennan et al.* (2005) show that both wave age and steepness formulations are of comparable performance for dominant wind-sea conditions, whereas for under-developed "young" wind sea the former is better and for mixed sea conditions the latter is better. The work presented in section 4 could be used to compare the performance of additional SL models (such as the wave steepness roughness scaling).

However, in general, SL model differences in terms of wind stress magnitude are small for winds below 10 m/s, and it is only well above 10 m/s that the different roughness formulations produce large differences in the estimated stress (see also *Taylor et al., 2001*). Moreover, according to *Bourassa* (2006), the most recently developed SL models have similar performance up to 16 m/s, which is consistent with the comparison of LKB and ECMWF SL models performed in section 3 (e.g., see Figure 2). However, cases of extreme wind variability or air-sea temperature difference may show large wind and stress discrepancies. The two-year extra-tropical triple collocated dataset was not sufficient to properly investigate the performance of the SL models in such extreme cases, where the differences between models may be more significant. As such, a study over a much larger dataset is recommended for such purposes. Moreover, it would also be interesting to study the ability of scatterometers to measure stress in such extreme conditions.

A new C-band scatterometer, i.e., ASCAT (onboard MetOp), which has more than twice the coverage of the ERS scatterometer, was launched on October 19, 2006. In the framework of a collaboration between the NOAA and EUMETSAT, ASCAT underflights are planned in both the NOAA 2007 winter storm and tropical cyclone campaigns. These extreme weather datasets could therefore be used for the above mentioned purposes.

Appendix: moored buoy data online

In the work described here and in *Stoffelen et al.* (2006), software is adapted and developed to process moored buoy data and perform triple collocations. Tropical buoy datasets are manually (interactively) collected online (see *Stoffelen et al., 2006*). However, because of the difficulties we encountered at the beginning of the project to retrieve online extra-tropical buoy data, GTS buoy data were used instead (see section 2).

Within the EUMETSAT SAFs, there are plans to monitor the performance of ASCAT through routine checks against NWP models and buoy data. However, it is not easy to automatically access the various buoy systems advertised online.

In this section, we explain our own experience in trying to get manual or automatic access to some of these systems.

TAO/TRITON and PIRATA buoy arrays:

Tropical Pacific (TAO/TRITON) and Atlantic (PIRATA) buoy data arrays are available online at *http://www.pmel.noaa.gov/tao/* and *http://www.pmel.noaa.gov/pirata/*, respectively. Archive data can be ordered online interactively through a friendly web interface. However, public access (via ftp) to the archive is not granted and, as such, there is no straightforward way to automatically collect the data.

NDBC buoy data:

NOAA's National Data Buoy Center (NDBC) site (*http://www.ndbc.noaa.gov/*) provides access to a wide range of moored buoy data around the globe, including the above mentioned TAO/TRITON and PIRATA data arrays, Irish buoys, Met Office buoys, etc. However, buoy data other than NOAA's are only available for the last 24 hours and not in electronic format. NDBC archived data can be ordered online on a buoy-by-buoy basis or can be automatically retrieved via the FTP site *ftp.ndbc.noaa.gov*. Unfortunately, since June 2006 access to the ftp site has been restricted.

In contrast with TAO/TRITON and PIRATA data, NDBC data files do not contain geographical location information and the sensor heights, which are not reported, can differ substantially among buoys. This information is actually quite relevant, since moored buoys can be sometimes moved to another location and/or their payload (including sensor height) changed. At the NDBC web site, there is a link to a "NDBC data inventory" where all the information on payload and location changes is reported. The information is however not provided in any readable format. Moreover, it has not been updated since 2003. An alternative for automatic data retrieval (provided that access to the ftp site is granted again) is to daily retrieve and store the file "station_table.txt". The latter is a daily report for all NDBC buoys in ASCII format, which includes geographical location and payload changes (among others).

In summary, software has been developed to process NDBC buoy data both manually and automatically. The former is based on the (manual) elaboration of a sensor height and location file (derived from the "NDBC data inventory" page) and the online retrieval (interactively) of yearly NDBC buoy data files; and the latter is based on the (automatic) retrieval of the "station_table.txt" file and the archived NDBC buoy data files available on the ftp site. As mentioned above, access to the ftp site is restricted and therefore only the manual stream can be operated for now.

Note that after writing this report, we have been informed that NDBC archived data, including sensor height and location information, are available at the following ftp site: ftp.nodc.noaa.gov. Observations up to the last complete month are available at this site and therefore suitable for monitoring purposes. In the future, we plan to automatically retrieve NDBC data from this ftp site for monitoring ASCAT.

Other buoy data online:

A thorough search for additional moored buoy data (other than the above mentioned US buoys) was conducted. The following web sites advertise buoy data containing (at least) sea surface wind vector, SST, and air temperature information (necessary parameters for the work described in this report): *http://www.metoffice.gov.uk/research/ocean/goos/maws_pic.html* (UK buoys); *http://www.marine.ie/home/publicationsdata/data/buoys/DataBuoyHome.htm* (Irish buoys); *http://www.puertos.es/index2.jsp?langId=2&catId=1024462535987&pageId=1053533857296* (Spanish buoys); *http://www.poseidon.ncmr.gr/* (Greek buoys); *http://www.vliz.be/NL/Datacentrum/MVB_intro* (Belgian buoys); and *http://www.niot.res.in/ndbp/* (Indian buoys).

None of these web sites provide buoy data online automatically nor manually (interactively). Data requests are off line either via registration and order forms or via e-mail. We requested buoy data via e-mail to the UK, Spanish, Belgian, and Greek sites a year ago and we only got an answer from the UK site, which sells (at a very high price) buoy data on request.

References

Attema, E. P. W., "The active microwave instrument on board the ERS-1 satellite," *Proc. IEEE*, vol. 79, pp. 791-799, 1991.

Beljaars, A.C.M., "Air-sea interaction in the ECMWF model," *Proc. of seminar on atmosphere-surface interaction*, European Centre for Medium-Range Weather Forecasts, Reading, United Kingdom, 1997.

Bidlot J.-R., D. J. Holmes, P. A. Wittmann, R. Lalbeharry, H. S. Chen, 2002: Intercomparison of the performance of operational ocean wave forecasting systems with buoy data. *Wea. Forecasting*, 17, 287-310.

Bonekamp, H., Komen, G.J., Sterl, A., Janssen, P.A.E.M., Taylor, P.K., and Yelland, M.J., "Statistical comparisons of observed and ECMWF modelled open ocean surface drag," *J. Phys. Oceanogr.*, vol. 32, pp. 1010-1027, 2002.

Bourassa, M.A., "Satellite-based observations of surface turbulent stress during severe weather," (Chapter 2), *Atmosphere-Ocean Interactions*, vol. 2, ed., W. Perrie, Wessex Institute of Technology, pp. 35-52, 2006.

Businger, J.A., "Turbulent transfer in the atmospheric surface layer," *Workshop on Micrometeorology*, Amer. Meteorol. Soc., pp. 67-100 1973

Businger, J.A., "Interactions of sea and atmosphere," *Rev. Geophys. Space Phys.*, vol. 13, pp. 720-822, 1975.

Charnock, H., "Wind stress on a water surface," Q. J. R. Meteorol. Soc., vol. 81, pp. 639-640, 1955.

Chelton D.B., and Schlax, M.G., "Global observations of oceanic Rossby waves," *Science*, vol. 272, pp. 234-238, 1996.

Chelton, D.B., Esbensen, S.K., Schlax, M.G., Thum, N., Freilich, M.H., Wentz, F.J., Gentemann, C.L., McPhaden, M.J., and Schopf, P.S., "Observations of coupling between surface wind stress and sea surface temperature in the eastern Tropical Pacific," *J. Climate*, vol. 14, pp. 1479-1498, 2001.

Chelton, D.B., Schlax, M.G., Freilich, M.H., Millif, R.F., "Satellite measurements reveal persistent small-scale features in ocean winds," *Science*, vol. 303, pp. 978-983, 2004.

Djepa, V., "Validation of the retrieved winds fields by ERS scatterometer over tropical ocean surface, Parts I and II," EUMETSAT Ocean and sea ice SAF VS report, available at http://www.eumetsat.int/Home/Main/What_We_Do/SAFs/The_Network/Visiting_Scientists_Programme/, 2001.

Donelan, M.A., "Air-sea interaction," in *The Sea*, vol. 9, *Ocean Engineering Science*, ed. LeMéhauté, B., and Hanes, D., pp. 239-292, John Wiley, New York, 1990.

Donelan, M.A., Dobson, F.W., Smith, S.D., and Anderson, R.J., "On the dependence of sea surface roughness on wave development," *J. Phys. Oceanogr.*, vol. 23, pp. 2143-2149, 1993.

Drennan, W.M., Graber, H.C., Hauser, D., Quentin, C., "On the wave age dependence of wind stress over pure wind seas," *J. Geophys. Res.*, vol. 108(C3), 8062, doi:10.1029/2000JC000715, 2003.

Drennan, W.M., Taylor, P.K., and Yelland, M.J., "Parameterizing the sea surface roughness," *J. Phys. Oceanogr.*, vol. 35, pp. 835-848, 2005.

Friehe, C.A., and Schmitt, K.F., "Parameterization of air-sea interface fluxes of sensible heat and moisture by bulk aerodynamic formulas," *J. Phys. Oceanogr.*, vol. 6, pp. 801-809, 1976.

Garrat, J.R., "Review of drag coefficients over oceans and continents," *Mon. Wea. Rev.*, vol. 105, pp. 915-929, 1977.

Geernaert, G.L., "Theory of air-sea momentum, heat and gas fluxes," in *Air-sea exchange: physics, chemistry, and dynamics*, ed. G.L. Geernaert, Kluwer Academy Publishers, Boston, pp. 25-48, 1999.

Hersbach, H., A. Stoffelen, and de Haan, S., "The improved C-band ocean geophysical model function CMOD-5", *J. Geophys. Res.*, vol. 112 (C3), doi:10.1029/2006JC003743, 2007.

Janssen, P., "The interaction of ocean waves and wind," *Cambridge University Press*, 300pp, 2004.

Johnson, H.K., Højstrup, J., Vested, H.J., Larsen, S.E., "On the dependence of sea surface roughness on wind waves," *J. Phys. Oceanogr.*, vol. 28, pp. 1702-1716, 1998.

Kelly, K.A., Dickinson, S., McPhaden, M.J., and Johnson, G.C., "Ocean currents evident in satellite wind data," *Geophys. Res. Lett.*, vol. 28(12), pp. 2469-2472, 2001.

Liu, W.T., Katsaros, K.B., and Businger, J.A., "Bulk parameterization of air-sea exchanges of heat and water vapor including the molecular constraints in the interface," *J. Atmos. Sci.*, vol. 36, 1979.

Liu, W.T., and Tang, W., "Equivalent neutral wind," *Jet Propulsion Laboratory 96-17*, Pasadena, USA, August 1996.

Maat, N., Kraan, C., and Oost, W.A., "The roughness of wind waves," *Boundary Layer Meteorol.*, vol. 54, pp. 89-103, 1991.

Milliff, R.F., "Forcing global and regional ocean numerical models with ocean surface vector winds from spaceborne observing systems," in *Proc. 2nd Ocean and Sea Ice SAF Workshop*, EUM P.45, ISBN 1561-1485, Perros-Guirec, France, 15-17 March, 2005.

Milliff, R.F., and Morzel, J., "The global distribution of the time-average wind stress curl from NSCAT," *J. Atmos. Sci.*, vol. 58 (2), 2001.

Monin, A.S., and Obukov, A.M., "Basic regularity in turbulent mixing in the surface layer of the atmosphere," *USSR Acad. Sci. Geophys. Inst.*, No 24, 1954.

Park, K.A., Cornillon, P., and Codiga, D., "Modification of surface winds near ocean fronts: effects of Gulf Stream rings on scatterometer (QuikSCAT, NSCAT) wind observations," *J. Geophys. Res.*, vol. 111, C03021, doi:10.1029/2005JC003016, 2006.

Pond, S., Fissel, D.B., and Paulson, C.A., "A note on bulk aerodynamic coefficients for sensible heat and moisture fluxes," *Boundary Layer Meteorol.*, vol. 6, pp. 333-340, 1974.

Smith, S.D., Anderson, R.J., Oost, W.A., Kraan, C., Maat, N., DeCosmo, J., Katsaros, K.B., Davidson, K.L., Bumke, K., Hasse, L., and Chadwick, H.M., "Sea surface wind stress and drag coefficients: the HEXOS results," *Boundary Layer Meteorol.*, vol. 60, pp. 109-142, 1992.

Stoffelen, A., "Scatterometer Ocean Stress," *proposal to the CM-SAF*, Koninklijk Nederlands Meteorologisch Instituut, The Netherlands, available at http://www.knmi.nl/scatterometer/, 2002.

Stoffelen, A., "Error modeling of scatterometer, in-situ, and ECMWF model winds; a calibration refinement," *Technical report TR-193*, Koninklijk Nederlands Meteorologisch Instituut, The Netherlands, 1996.

Stoffelen, A., "Scatterometry," *PhD thesis at the University of Utrecht*, ISBN 90-393-1708-9, October 1998a.

Stoffelen, A., 'Error modeling and calibration: towards the true surface wind speed," *J. Geophys. Res.*, vol. 103, no. C4, pp. 7755-7766, 1998b.

Stoffelen, A., Van Oldenborgh, G.J., De Kloe, J., Portabella, M., and Verhoef, A., "Development of a scatterometer ocean stress product," report for the EUMETSAT Climate Monitoring SAF, 2006.

Taylor, P.K., and Yelland, M.J., "The dependence of sea surface roughness on the height and steepness of the waves," *J. Phys. Oceanogr.*, vol. 31, pp. 572-590, 2001.

Taylor, P.K., Yelland, M.J., and Kent, E.C., "On the accuracy of ocean winds and wind stress," *WCRP/SCOR Workshop on Intercomparison and Validation of Ocean-Atmosphere Flux Fields*, Bolger Center, Potomac, MD, USA, May 2001.

Vialard, J., "Seasonal forecast and its requirements for satellite products," *Proc. OSI SAF training workshop*, ISBN 92-9110-034-X, EUMETSAT P27, Darmstadt, Germany, pp. 137-143, 2000.

Yelland, M.J., Moat, B.I., Taylor, P.K., Pascal, R.W., Hutchings, J., and Cornell, V.C., "Measurements of the open ocean drag coefficient corrected for air flow disturbance by the ship," *J. Phys. Oceanogr.*, vol. 28, pp. 1511-1526, 1998.

Acknowledgements

We acknowledge the help and collaboration of our colleagues working at KNMI, and more in particular the people from the scatterometer group. Special thanks go to Jean-Raymond Bidlot and ECMWF for providing the GTS buoy dataset (already quality controlled) together with some additional feedback needed for the collocation exercise. This work is funded by the European Meteorological Satellite Organization (EUMETSAT) Ocean & Sea Ice (OSI) Satellite Application Facilities (SAF), lead by Météo France. The software used in this work has been developed at KNMI, through the EUMETSAT OSI and Numerical Weather Prediction (NWP) SAFs, and at ECMWF.